

University of Mississippi

eGrove

Honors Theses

Honors College (Sally McDonnell Barksdale
Honors College)

Spring 5-13-2023

An Analysis of Detection Asymmetry Using Baryon Decays in Belle II

Matthew Mestayer

Follow this and additional works at: https://egrove.olemiss.edu/hon_thesis



Part of the [Elementary Particles and Fields and String Theory Commons](#)

Recommended Citation

Mestayer, Matthew, "An Analysis of Detection Asymmetry Using Baryon Decays in Belle II" (2023). *Honors Theses*. 2976.

https://egrove.olemiss.edu/hon_thesis/2976

This Undergraduate Thesis is brought to you for free and open access by the Honors College (Sally McDonnell Barksdale Honors College) at eGrove. It has been accepted for inclusion in Honors Theses by an authorized administrator of eGrove. For more information, please contact egrove@olemiss.edu.

AN ANALYSIS OF DETECTION ASYMMETRY USING BARYON DECAYS IN
BELLE II

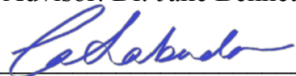
by
Matthew Mestayer

A thesis submitted to the faculty of The University of Mississippi in partial fulfillment of the
requirements of the Sally McDonnell Barksdale Honors College.

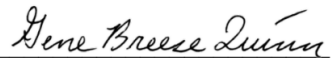
Approved by:



Advisor: Dr. Jake Bennett



Reader: Dr. Cecille Labuda



Reader: Dr. Breese Quinn

© 2023
Matthew Mestayer
ALL RIGHTS RESERVED

Abstract

The purpose of this study was to determine the detection asymmetry of the Belle II detector using decays of two common baryons, $\Lambda^0 \rightarrow p\pi^-$ and $\Sigma^+ \rightarrow p\pi^0$. A Monte Carlo simulation of both decays was used to determine the validity of signal isolation criteria. These criteria were then applied to the Belle II data, allowing for a comparison of the detection asymmetry in the data relative to the simulation. The results show a moderate detection asymmetry when using the $\Lambda^0 \rightarrow p\pi^-$ decay, particularly for forward-going baryons. For the $\Sigma^+ \rightarrow p\pi^0$ decay, a more significant asymmetry is observed, irrespective of the angular direction. These results demonstrate potential asymmetries in either detection or production that must be accounted for in future studies.

Table of Contents

| | |
|---|----|
| List of Figures..... | v |
| Acknowledgements..... | vi |
| 1: Introduction..... | 1 |
| 2: Methods..... | 12 |
| 2.1: Monte Carlo simulations and sWeights..... | 13 |
| 2.2: $\Lambda^0 \rightarrow p\pi^-$ and $\Sigma^+ \rightarrow p\pi^0$ decays..... | 21 |
| 3: Results..... | 22 |
| 4: Discussion..... | 29 |
| Bibliography..... | 31 |

List of Figures

| | | |
|------------|---|----|
| Figure 1.1 | Standard Model diagram..... | 2 |
| Figure 1.2 | Quark Diagram of $\Lambda^0 \rightarrow p\pi^-$ | 3 |
| Figure 1.3 | Quark Diagram of $\Sigma^+ \rightarrow p\pi^0$ | 4 |
| Figure 1.4 | $\Lambda^0 \rightarrow p\pi^-$ in electron-positron event..... | 6 |
| Figure 1.5 | $\Sigma^+ \rightarrow p^+\pi^0$ in electron-positron event..... | 6 |
| Figure 1.6 | Diagram of the SuperKEKB collider..... | 9 |
| Figure 1.7 | Diagram of the Belle II detection chamber..... | 10 |
| Figure 2.1 | Example of mass plot of Λ^0 | 15 |
| Figure 2.2 | Example of mass plot of Σ^+ | 16 |
| Figure 2.3 | MC fitting for Λ^0 mass..... | 17 |
| Figure 2.4 | Data Fitting for Λ^0 mass..... | 18 |
| Figure 2.5 | MC fitting for Σ^+ mass..... | 19 |
| Figure 2.6 | Data Fitting for Σ^+ mass..... | 20 |
| Figure 3.1 | Plot of the angular displacement of the Λ^0 baryon..... | 23 |
| Figure 3.2 | Plot of the angular distribution between Λ^0 and $\bar{\Lambda}^0$ for signal MC..... | 24 |
| Figure 3.3 | Plot of the angular displacement of the Σ^+ baryon..... | 25 |
| Figure 3.4 | Plot of the angular distribution between Σ^+ and $\bar{\Sigma}^+$ for signal MC..... | 26 |
| Figure 3.5 | A final measure of the the Λ^0 detection asymmetry..... | 27 |
| Figure 3.6 | A final measure of the the Σ^+ detection asymmetry..... | 28 |

To Dr. Jake Bennett for his expertise and advice

To Anil Panta for his support

1: Introduction

The Standard Model of particle physics is currently the most successful attempt at describing the fundamental characteristics of subatomic particles. It describes six quark flavors, along with their six antimatter partners and outlines how these quarks interact. A diagram detailing the Standard Model is given in Figure 1.1. These interactions are predicated upon certain symmetries and conservation rules, such as the conservation of momentum and energy. One quantity that was originally believed to be conserved is called CP symmetry, which essentially explains the difference in behavior of antiparticles relative to their particle counterparts. Charge conjugation describes the effect of changing each particle into its antimatter partner, or vice versa. Parity describes the effect of reversal of the spatial directions. The combination of parity and charge conjugation, CP, can be violated under certain conditions, as demonstrated by Madame Wu in 1957 [1].

CP violation is an essential ingredient for baryogenesis, the development of a matter-only universe after equal parts of matter and antimatter were created after the big bang. However, the amount of CP violation described by the Cabibbo-Kobayashi-Maskawa mechanism in the standard model is insufficient for that process. An example of particle decays, which involves quark mixing, is shown in Figures 1.2 and 1.3. In each of the diagrams, a particle decay involves the production or transformation of quarks. A change in quark flavor (or type) involves the emission of a W^+ boson, which then creates additional quarks. The type of flavor change is related to the probability for the reaction to occur. If CP is conserved, the rate should be the same

Standard Model of Elementary Particles

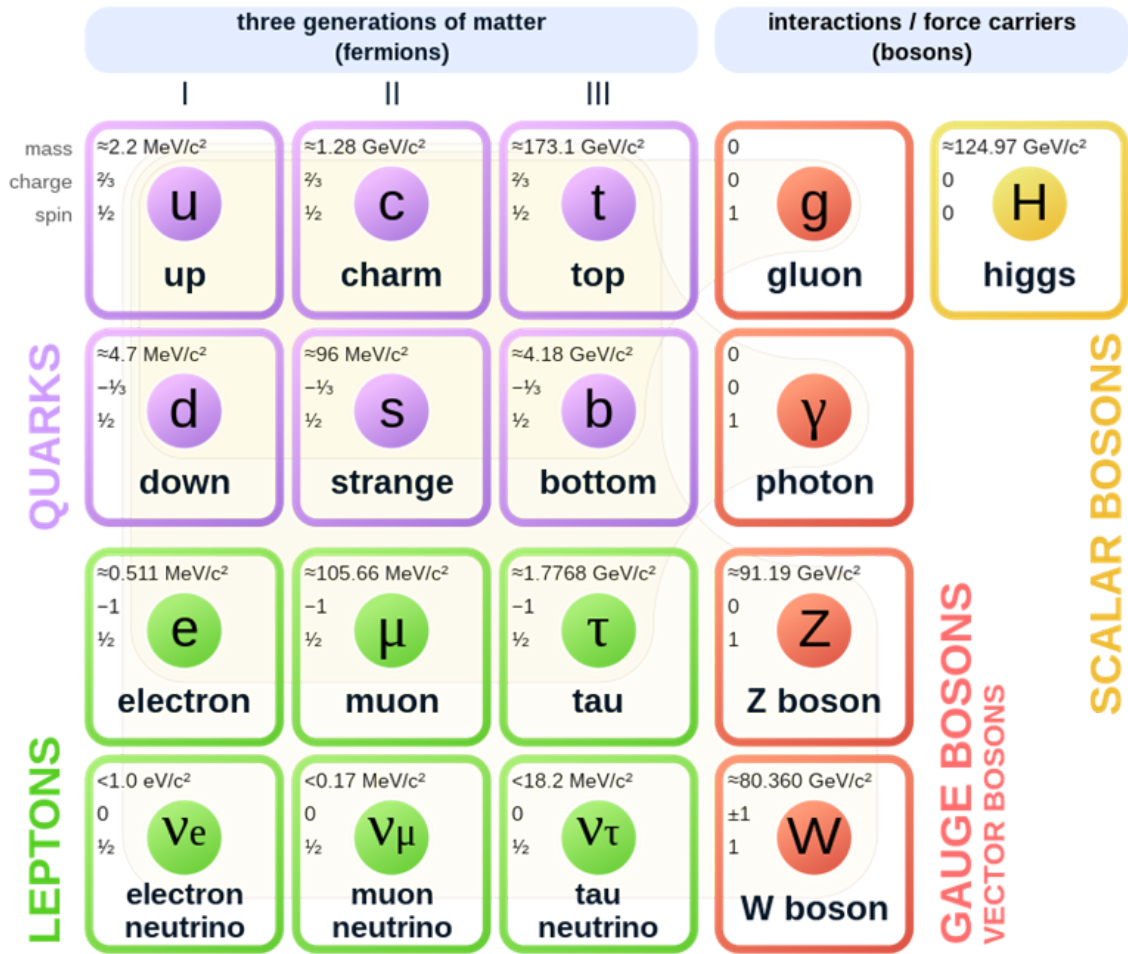


Figure 1.1 - Diagram of Standard Model of Particle Physics. The six flavors of quarks are represented by the purple section. In certain cases, these quarks can change flavors. Particles composed of three quarks or antiquarks are baryons and particles composed of a quark and antiquark are mesons.

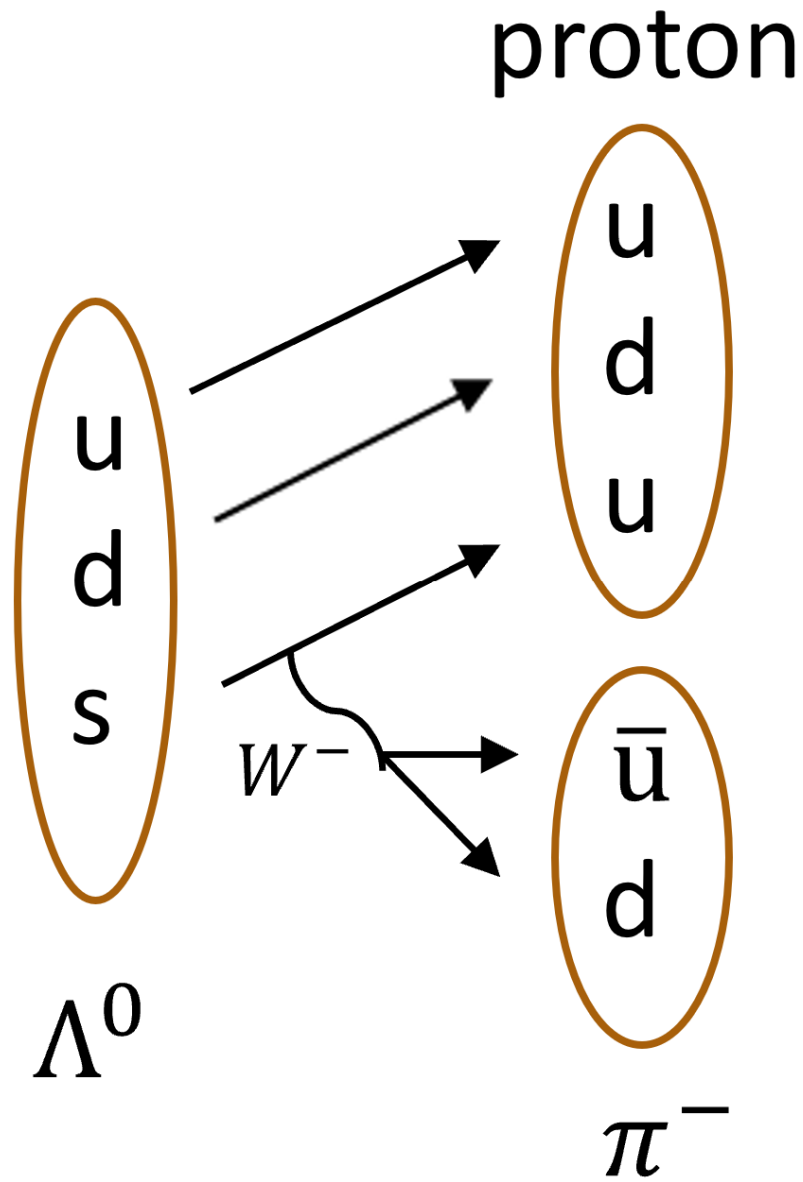


Figure 1.2 - Quark Diagram of $\Lambda^0 \rightarrow p\pi^-$. The Λ^0 baryon (uds) decays into a proton (udu) and a negative pion ($\bar{u}d$). This is allowed since the strange quark decays into the up quark, emitting a negative W boson in the process to form the negative pion.

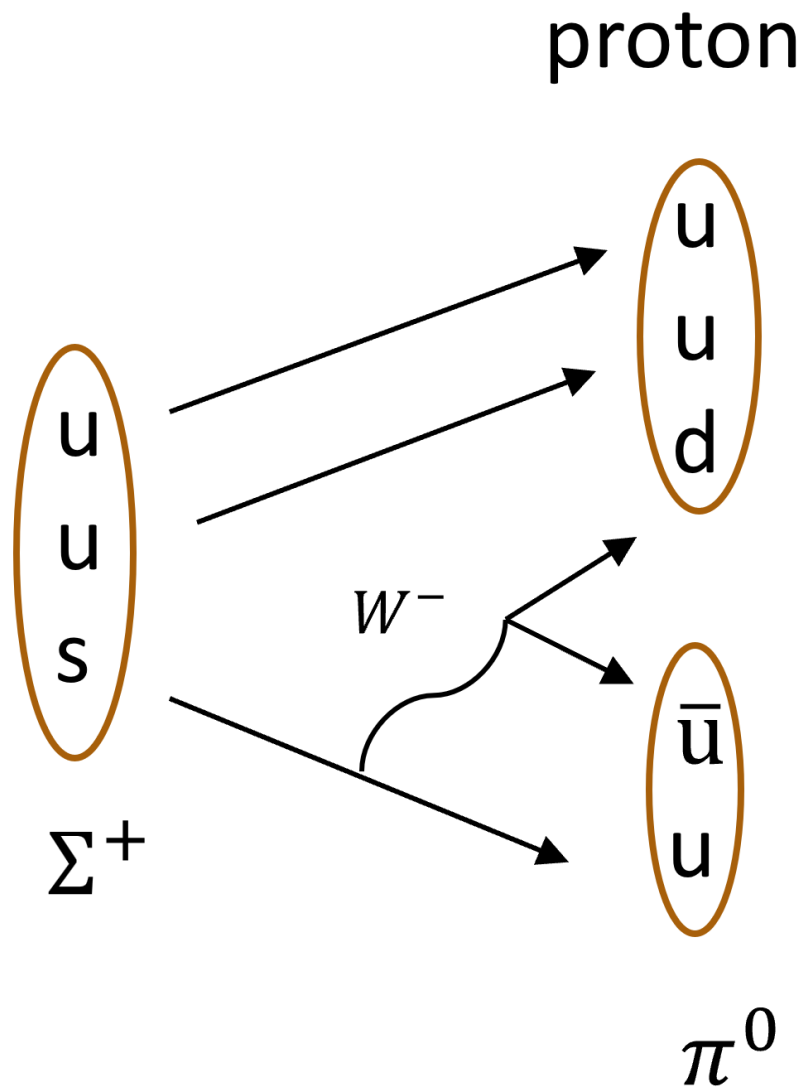


Figure 1.3 - Quark Diagram of $\Sigma^+ \rightarrow p\pi^0$. The Σ^+ baryon (uus) decays into a proton (udu) and a neutral pion ($\bar{u}u$). Like the Λ^0 decay, this is allowed since the strange quark decays into the up quark, emitting a negative W boson in the process.

whether the quarks involved are matter or antimatter. By measuring such rates very precisely, it is possible to test the predicted amount of CP violation according to the standard model.

One major goal of the Belle II experiment is to search for new sources of CP violation, beyond the standard model of particle physics. One environment conducive to this is in charm baryon decays, which have not been studied in great detail to date. The expected amount of CP violation in the charm sector is very small according to the Standard Model, so any sizable observation could be an indication of physics beyond the standard model.

The Belle II experiment is based at the SuperKEKB collider, located in Tsukuba, Japan. Together, the detector and collider represent a major upgrade of the previous Belle experiment at the KEKB collider. The Belle experiment was one of two experiments to discover CP violation in the B-meson system (the other experiment was BaBar, which made a simultaneous discovery). The SuperKEKB electron-positron collider will enable a continuation of the very successful B-factory physics program by providing an instantaneous luminosity about 40 times that of KEKB [2]. This increased luminosity allows for precision studies of suppressed and rare decays, in which signatures for new physics may be discovered.

The Belle II group at the University of Mississippi is using the Belle II data sample to study charmed baryons, which include a charm quark along with two light quarks (up, down, or strange), specifically to search for CP violation. Example decay processes being studied are given by Figures 1.4 and 1.5. Beam bunches of electrons and positrons are accelerated close to the speed of light in the SuperKEKB accelerator and then collide at the center of the Belle II detector. The energy released in the collision is converted into particles, such as the Ξ_c^+ , which then decay into “final state” particles. Charmed baryons will eventually produce at least one proton due to

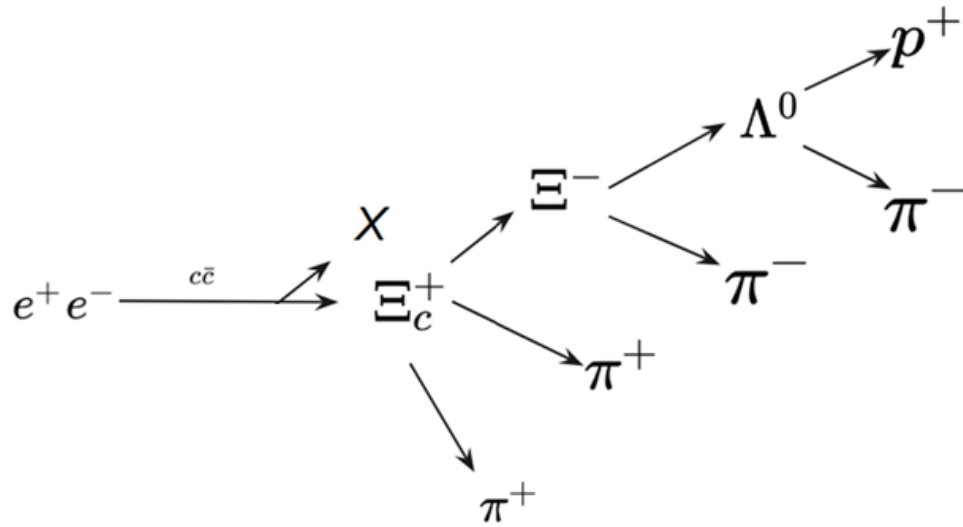


Figure 1.4 - Example of event after an electron-positron collision inside Belle II detector. Included in this decay is the $\Lambda^0 \rightarrow p\pi^-$ decay.

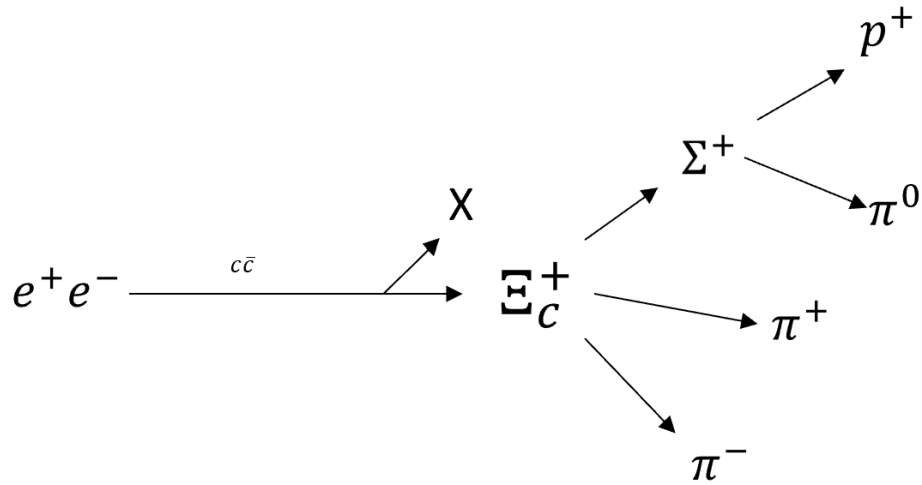


Figure 1.5 - Example of event after electron-positron collision inside the Belle II detector. Included is decay of $\Sigma^+ \rightarrow p^+ \pi^0$.

conservation of baryon number. The total number of baryons minus the number of antibaryons must remain constant in any decay. Two baryon decays that occur frequently are $\Lambda^0 \rightarrow p\pi^-$ and $\Sigma^+ \rightarrow p\pi^0$, which have branching ratios of 63.9% and 51.57% of decays for the Λ^0 and Σ^+ baryons, respectively [3]. Both the Λ^0 and Σ^+ are baryons (not antibaryons), and therefore both decay into protons (not antiprotons). Conversely, the $\bar{\Lambda}^0$ and $\bar{\Sigma}^-$ are antibaryons, and therefore decay into antiprotons (not protons). The protons and pions resulting from these decays are particles that will not decay further within the detector. Since no CP violation is expected for these decays, they are therefore an excellent source with which to study the detector performance with clean samples of protons and antiprotons. If the detector preferentially measures one over the other, it creates a fake source of CP violation purely through the asymmetry in detection. For this study, unless otherwise specified, it is implied that the charge conjugate decay is also included for a given reaction.

Figure 1.6 outlines the structure of the SuperKEKB electron-positron collider. The beams collide within the Belle II detector, where data from the collision is collected. As indicated by Figure 1.7, the Belle II detector consists of various sub-detector systems arranged in a cylindrical pattern around the axis defined by the electron and positron beams. One important component of the detector is the Central Drift Chamber (CDC), which consists of layers of wires suspended in HeC_2H_6 [3] gas, which is easily ionized by charged particles. The wires, some of which are held at ground (field wires) and others of which are held at a constant potential (sense wires), create an electric field, causing electrons to accelerate toward the sense wire. This begins an avalanche effect whereby additional electrons drift towards the wires. The resulting shower of electrons is detected as a potential drop in the sense wires. This results in a signal that indicates the passage of a charged particle within the “drift cell” defined by the field wires. The Lorentz force due to a uniform magnetic field created by a solenoid magnet causes the particles to curve according to their momentum. The Lorentz force, given by $F_{Lorentz} = qvB\sin\theta$ creates a centripetal force,

$F_{centripetal} = \frac{mv^2}{r}$. Setting the two equal and canceling terms gives $p = qrB$, where q is the particle charge, r is the radius of the particle's motion transverse to the magnetic field, B . Using the known values of the B field magnitude and the measured curvature of a particle, it is then possible to calculate the particle momentum.

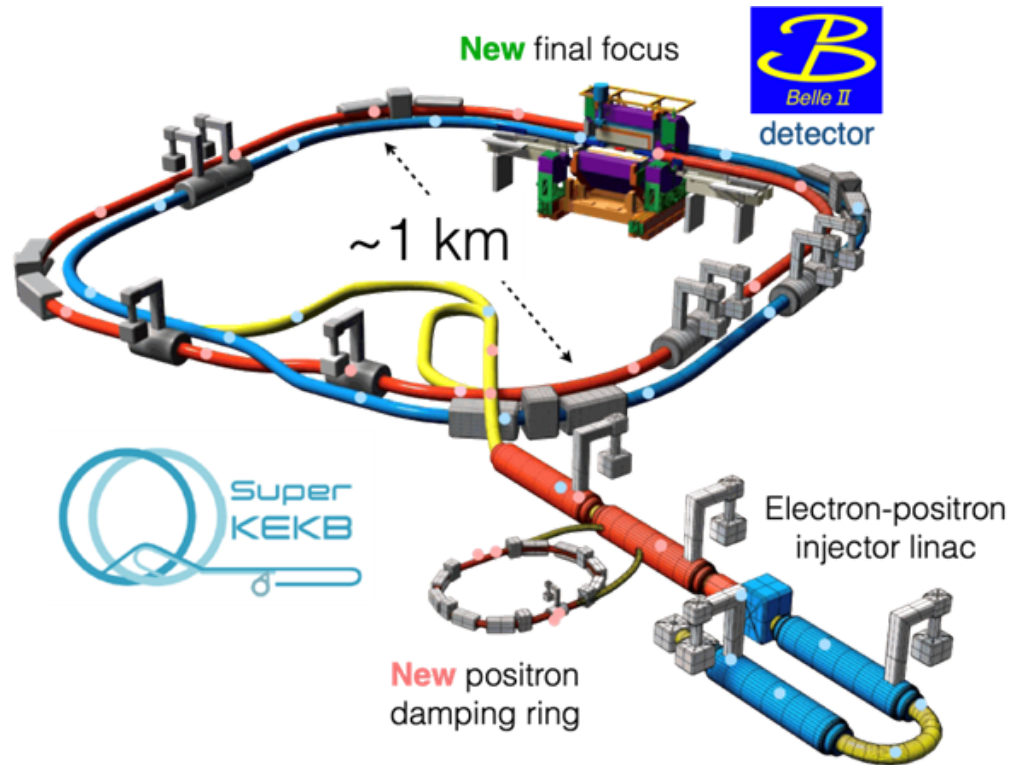


Figure 1.6 - Diagram of the SuperKEKB collider. Labeled here is the electron-positron injector, where the electron-positron beam is produced. The positron damping ring decreases the magnitude of the positron beam, resulting in an asymmetric beam. The beams then enter the rings, colliding in the Belle II detector.

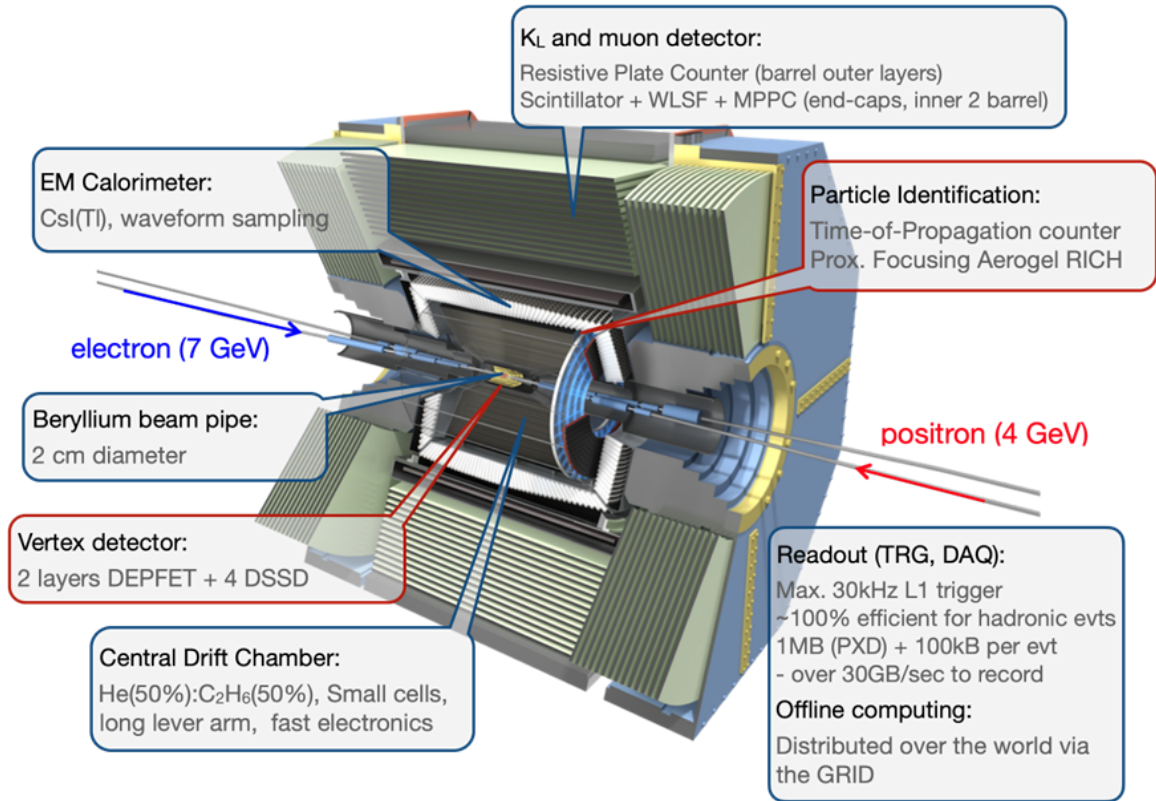


Figure 1.7 - A diagram of the Belle II detection chamber where electron-positron collisions occur. The EM Calorimeter detects the energy of photons and electrons produced by the collision, the Beryllium beam pipe heavily reduces background from soft synchrotron X-rays emitted by the beam due to beam acceleration, the Silicon vertex detector works in tandem with the Pixel Detector to reconstruct particle tracks, the K_L and muon detector detects any particles that escape detection from the other subdetectors, such as muons, and the Aerogel Ring-Imaging Cherenkov detector uses Cherenkov photons to determine the radius of particle tracks, providing a secondary source for particle identification.

Another important detector component is the Time of Propagation (TOP) chamber, which identifies the species of charged tracks. The TOP detector consists of quartz bars that have a high index of refraction. When charged particles travel faster than the phase velocity of light in a medium, the speed of light divided by the index of refraction, electromagnetic radiation is produced via the Cherenkov effect. The angle at which the light is produced is directly related to the velocity of the particle. Along with the momentum measurement by the CDC, this allows for a measurement of the mass of the particle and therefore its identity. Since the particle travels through the quartz with distance $x_{particle} = v_{particle} t$, and the emitted photon travels distance

$x_{photon} = v_{photon} t = \frac{ct}{n}$. The cosine of the angle between the two paths is given as

$\cos\theta = \frac{ct}{nv_{particle}t} = \frac{c}{nv_{particle}}$, where c is the speed of light in a vacuum, n is the refractive index of

the quartz, and $v_{particle}$ is the velocity of the particle through the quartz. By determining the velocity and momentum of the particle, the mass and thus the identity of the particle can be determined.

The particles that are detected by the Belle II detectors are the final state products of the electron-positron collision. These decays can be “reconstructed” using information gathered from the various subdetectors, such as the momentum and velocity of each particle. All of the reconstructed information can be combined to study any reaction of interest.

2: Methods

As discussed in the earlier sections, CP asymmetry measurements must take into account asymmetries created by Standard Model interactions, e.g. the interaction of a proton with electric fields in the CDC. The raw asymmetry measured by the detector can be represented by $A_{raw} = A_{CP} + A_{production} + A_{detector}$, where A_{CP} is the CP asymmetry, $A_{production}$ is an asymmetry due to production, and $A_{detector}$ is the detection asymmetry. It is perfectly expected that particles and antiparticles interact differently with this detector, which is made of matter and not antimatter. The resulting detector asymmetry results in a bias in the raw asymmetry that must be accounted for or else it can create fake CP violation measurements. Therefore, the asymmetry due to detector effects must be well understood.

By comparing the detection rate between baryons and antibaryons, a quantifiable asymmetry in detection can be accurately measured. However, events in the Belle II data contain far more than just Λ^0 and Σ^+ baryons in isolation. Many other particles are produced in the electron-positron collision, resulting in measured particles that do not come from a Λ^0 or Σ^+ decay. For the purposes of this study, the events that do not contain baryons of interest, henceforth referred to as background, must be removed from the data sample by applied selection criteria on the reconstructed information to study the detection asymmetry for the baryons of interest. A significant source of background is caused by misidentification, in which a final state decay ($p\pi^-$) is incorrectly attributed to a particle other than the particle of interest [4]. In this case, applying simple selection criteria will not suffice since the background events will be interpreted

as signal events. Instead, a statistical method must be employed to account for the effects of any remaining backgrounds, as described below.

2.1: Monte Carlo simulations and sWeights

Monte Carlo (MC) simulations produce events that can be compared to real data. MC simulations are commonly used within the field of high energy physics, mainly to determine selection criteria and to model the effect of new or important processes. For this experiment, the MC simulation includes generation of particles from the electron positron collision, their subsequent interactions with the Belle II detector, and the detector response [3]. The result is a simulated data sample that can be directly compared to real Belle II data. Selection criteria can be determined with MC samples since the “truth information” (i.e. whether a track was created by a muon or pion, the true mass and momentum of the particle, etc.) is known. Typically, MC files are generated with a size multiple times larger than the data sample of interest to minimize uncertainty due to MC statistics. To generate this MC sample, a decay file was written to describe the particular decays that are to be generated.

To generate signal MC, or MC which contain only events of interest, in this case $\Lambda^0 \rightarrow p\pi^-$ and $\Sigma^+ \rightarrow p\pi^0$, the HTCondor batch system in the University of Mississippi physics department was used. This cluster is controlled by a head node, umiss001. Instructions on what MC file will be made must be submitted to this head node, which then coordinates production using nodes from the entire cluster. The software used by the head node to distribute jobs is HTCondor, a software specializing in managing computationally intensive jobs, such as generating MC samples. Production of “generic MC” samples that include not just the decays of interest, but any possible decay, requires the use of the massive computing resources of the Belle II grid. These samples are centrally produced by the Data Production team and can be analyzed

by any Belle II member. Since I did not have access to these resources, my advisor used my code to run over the generic MC sample and downloaded the files for further, local analysis.

While backgrounds are reduced using event selection criteria, the remaining events can be statistically subtracted using the sPlot formalism, which aims to unfold distributions of mixed event samples into distinct categories [5]. A discrimination distribution, for which the identity of an event can be determined, is used to classify events according to a statistical probability to be either background or signal events. These probabilities can then be used to isolate the signal events for any control distribution, for which such classification is not possible. In this study, the discrimination variable is the mass of the mother particle, since the signal is expected to peak near the true mass of the particle and the background is expected to be flat as a function of mass, as shown in Figure 2.1. By fitting a probability density function (pdf) to a data sample, the probability for any event to be signal or background can be extracted. This probability can then be used to identify the signal for any other distribution, as described below.

For this study, the sPlot technique is used to calculate event weight factors, called sWeights. A fit is performed to the invariant mass distribution using a pdf consisting of a double Gaussian shape to describe the signal and a polynomial to describe the background, as shown in Figure 2.3. The fit is performed using a python-based fitting program called zFit [6]. The sWeights are then calculated from the results of the fit using a package called HEPStats [7]. Events that are likely to be signal (in the signal region) are given a positive weight, while those that are likely to be background are given a negative weight. These sWeights can then be applied on an event-by-event basis when plotting a control distribution, such as angular distributions. The negatively weighted background events that land outside the signal region from the mass plot will cancel the effect of the positively weighted background events that land within the signal region of the mass plot. The resulting distribution therefore only includes the effect of the signal events.

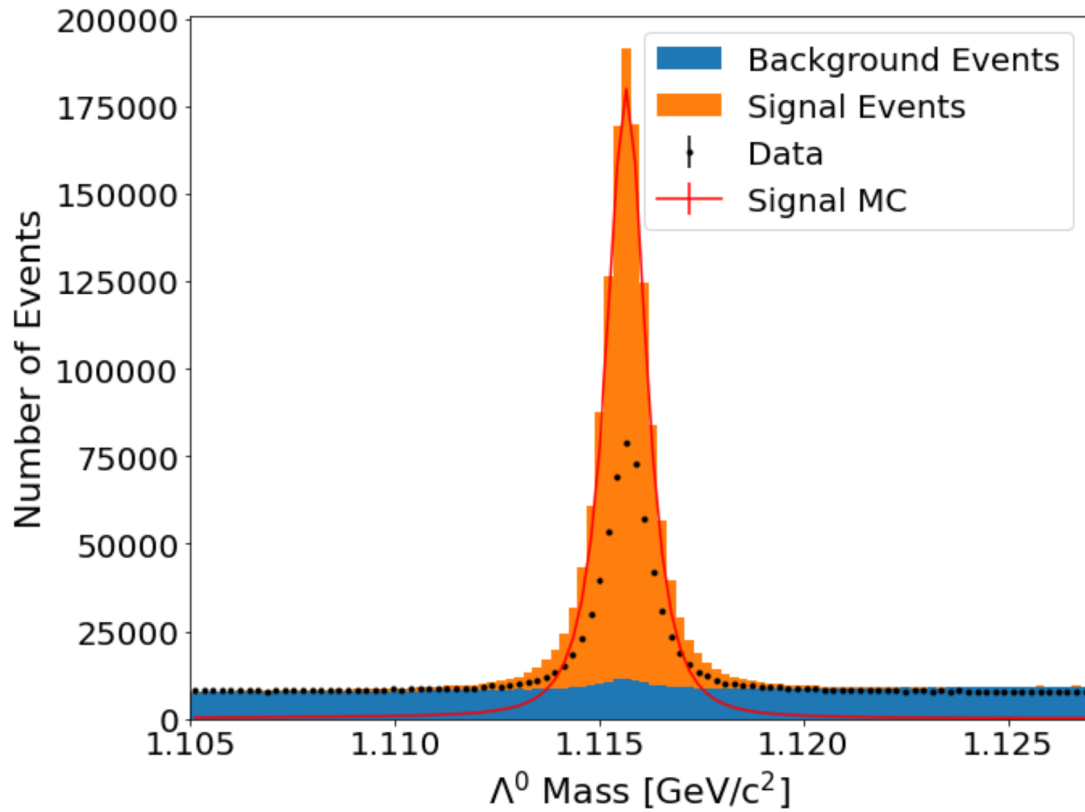


Figure 2.1 - Example of mass plot of Λ^0 . The blue histogram represents the background according to truth information and the orange represents the signal when stacked on top of the background. The red line shows the signal alone, while the black markers show the data. A clear discrepancy in the number of signal events in the data relative to the MC sample is apparent. This distribution also includes antibaryon events ($\bar{\Lambda}^0 \rightarrow \bar{p} \pi^+$).

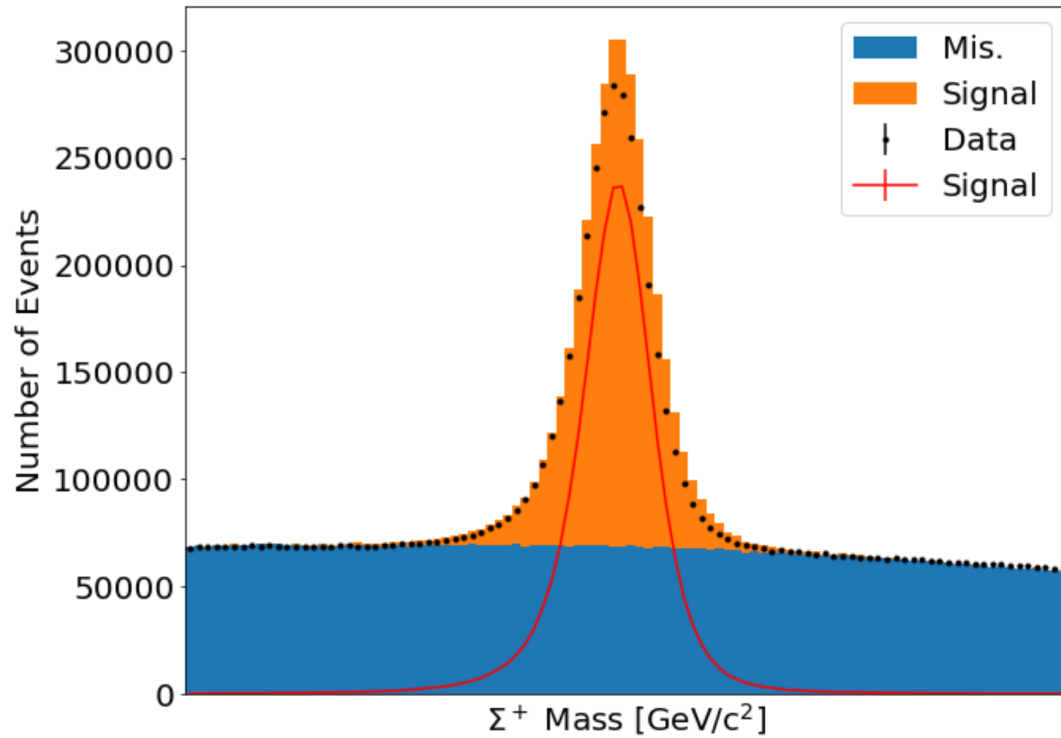


Figure 2.2 - Example of mass plot of Σ^+ . The blue histogram represents the background according to truth information and the orange represents the signal when stacked on top of the background. The red line shows the signal alone, while the black markers show the data. A clear discrepancy in the number of signal events in the data relative to the MC sample is apparent. This distribution also includes antibaryon events ($\bar{\Sigma}^- \rightarrow \bar{p} \pi^0$).

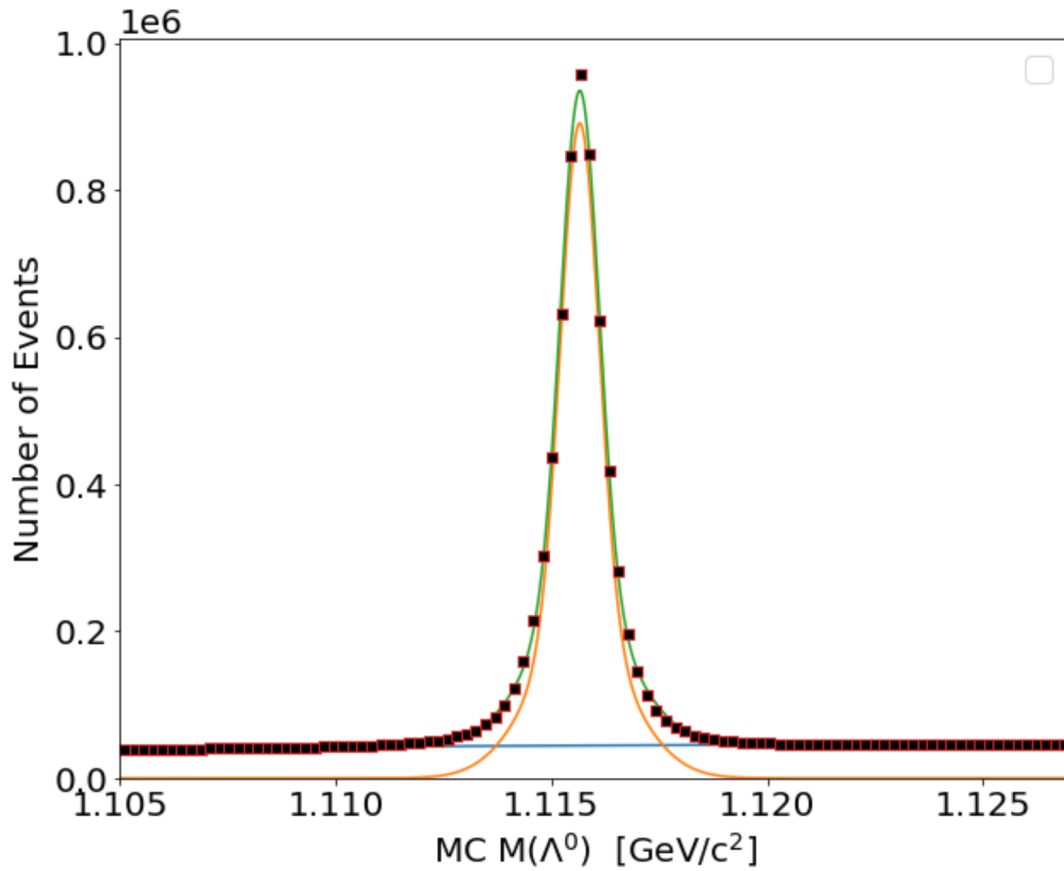


Figure 2.3 - Fitting for Λ^0 mass from MC. The black squares represent events from the MC file, the green curve represents the double Gaussian fit applied to the sample, the orange curve shows the signal distribution according to the fit, and the blue curve shows the polynomial fit applied to the background distribution.

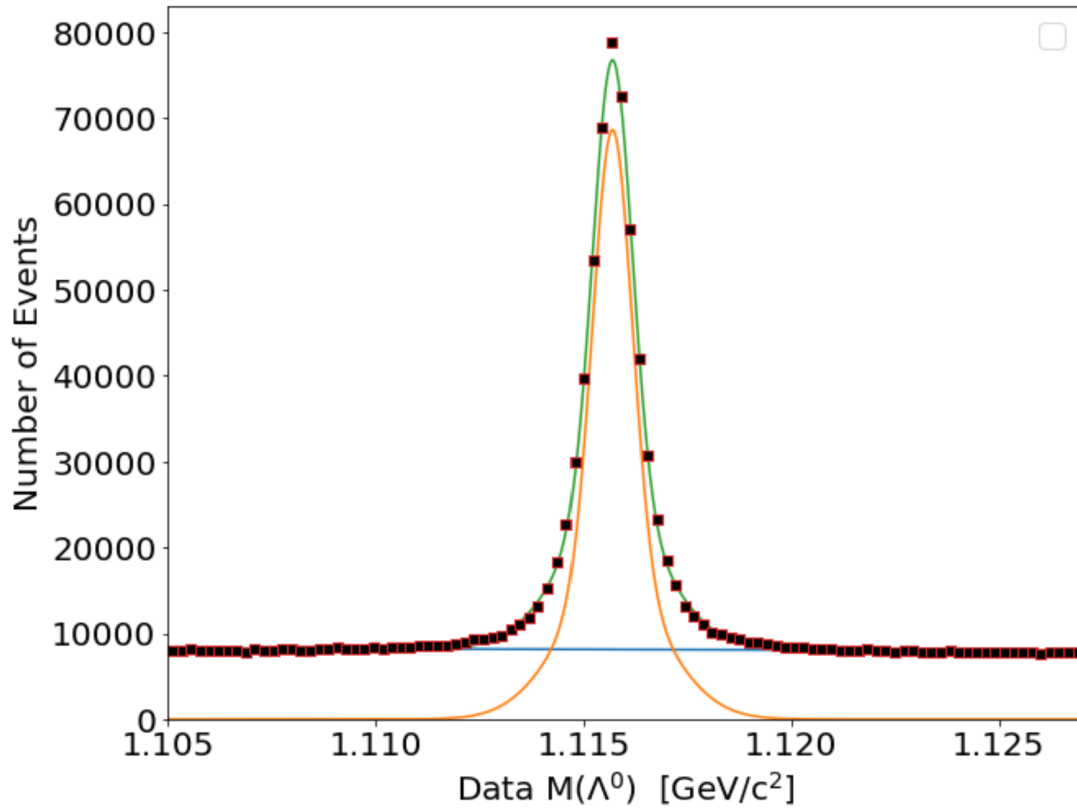


Figure 2.4 - Fitting for Λ^0 mass from data. The black squares represent events from the MC file, the green curve represents the double Gaussian fit applied to the sample, the orange curve shows the signal distribution according to the fit, and the blue curve shows the polynomial fit applied to the background distribution.

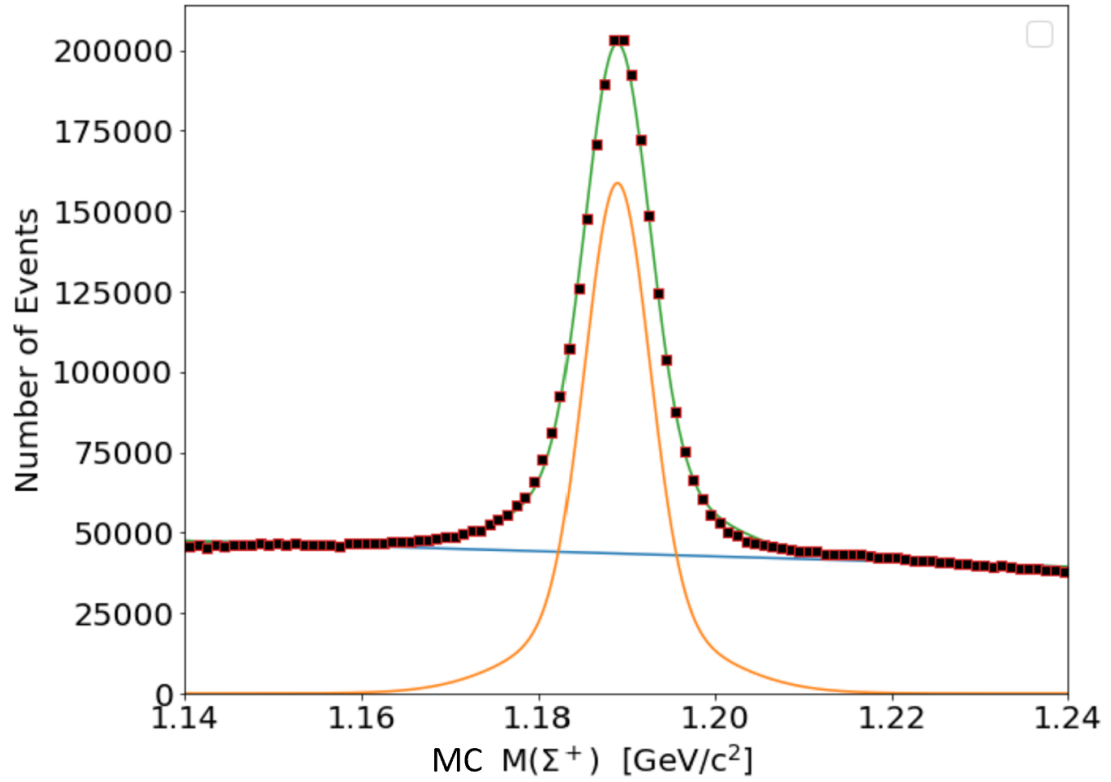


Figure 2.5 - Fitting for Σ^+ mass from MC. The black squares represent events from the MC file, the green curve represents the double Gaussian fit applied to the sample, the orange curve shows the signal distribution according to the fit, and the blue curve shows the polynomial fit applied to the background distribution.

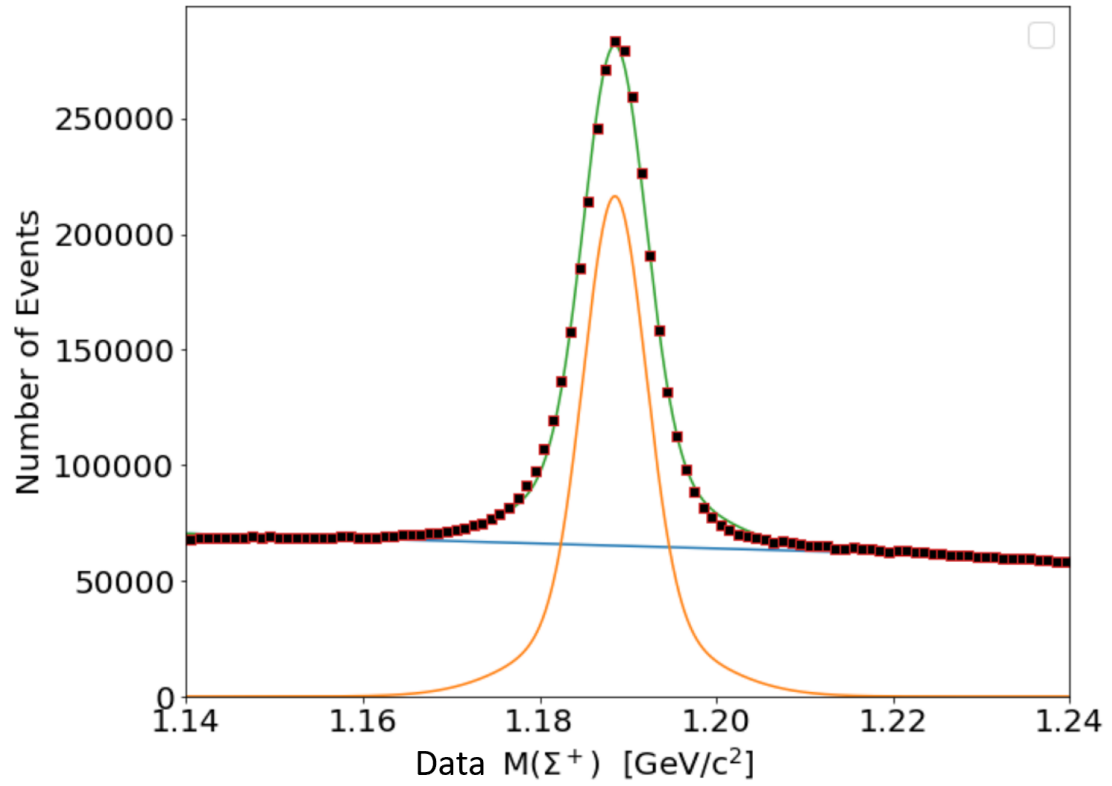


Figure 2.6 - Fitting for Σ^+ mass from data. The black squares represent events from the MC file, the green curve represents the fit applied to the sample, the orange curve shows the double Gaussian signal fit, and the blue curve shows the background distribution.

2.2: $\Lambda^0 \rightarrow p\pi^-$ and $\Sigma^+ \rightarrow p\pi^0$ decays

For both events of interest, the MC and data mass plots both had fits applied to them, with the corresponding sWeights being calculated from the fits. To locate this detector asymmetry in the detector, the events of interest were plotted as a function of $\cos(\theta)$, which is measured relative to the electron beam direction. After applying weights, the MC and signal sample show strong agreement in the $\cos(\theta)$ plots. Due to the MC sample containing more events than the data file, the MC size was adjusted until agreement was found between the signal MC, weighted MC, and weighted data. Then, the raw asymmetry between both decays was then calculated and plotted with respect to $\cos(\theta)$, allowing for a direct calculation of the raw asymmetry in the detector.

3: Data/Results

For this experiment, the weighted MC, signal MC, unweighted MC, and weighted data were plotted on the same plots. This allowed us to “test” the accuracy of the sPlot technique. These plots contain unofficial Belle II data. The results have not been officially approved by the Belle II collaboration. While they do contain accurate data, the results of this study still require verification. In Figure 3.1, the weighted data and signal MC display a strong agreement. In a sense, this allows me to “test” the sPlot technique. Since the signal MC and weighted MC are derived from the same MC file, they contain the same number of events and thus match well. For the data, the amount of events sampled differed from the MC, which resulted in a mismatch. A custom scale factor was applied to the MC to ensure the MC and data line up. To find the raw asymmetry, the number of events affiliated with the event of interest and the number of events affiliated with the antibaryon counterpart to this event was determined. Then, the equation

$$A_{detector} = \frac{N(\Lambda^0) - N(\bar{\Lambda}^0)}{N(\Lambda^0) + N(\bar{\Lambda}^0)},$$

where N refers to the number of events that were associated with the

particle of interest, was used to calculate the asymmetry. For no raw asymmetry, $N(\Lambda^0) = N(\bar{\Lambda}^0)$.

The variable $N(\Lambda^0)$ represents the asymmetry in the Λ^0 , but this same equation was used for the Σ^+ baryon. The asymmetries are depicted in Figures 3.5 and 3.6. Figures 3.2 and 3.4 depicts the

Λ^0 and $\bar{\Lambda}^0$ and Σ^+ and $\bar{\Sigma}^-$ $\cos(\theta)$ distributions for the Signal MC. Figures 3.2 and 3.4 were

included to demonstrate the baryon composition of the Signal MC in Figures 3.1 and Figures 3.3.

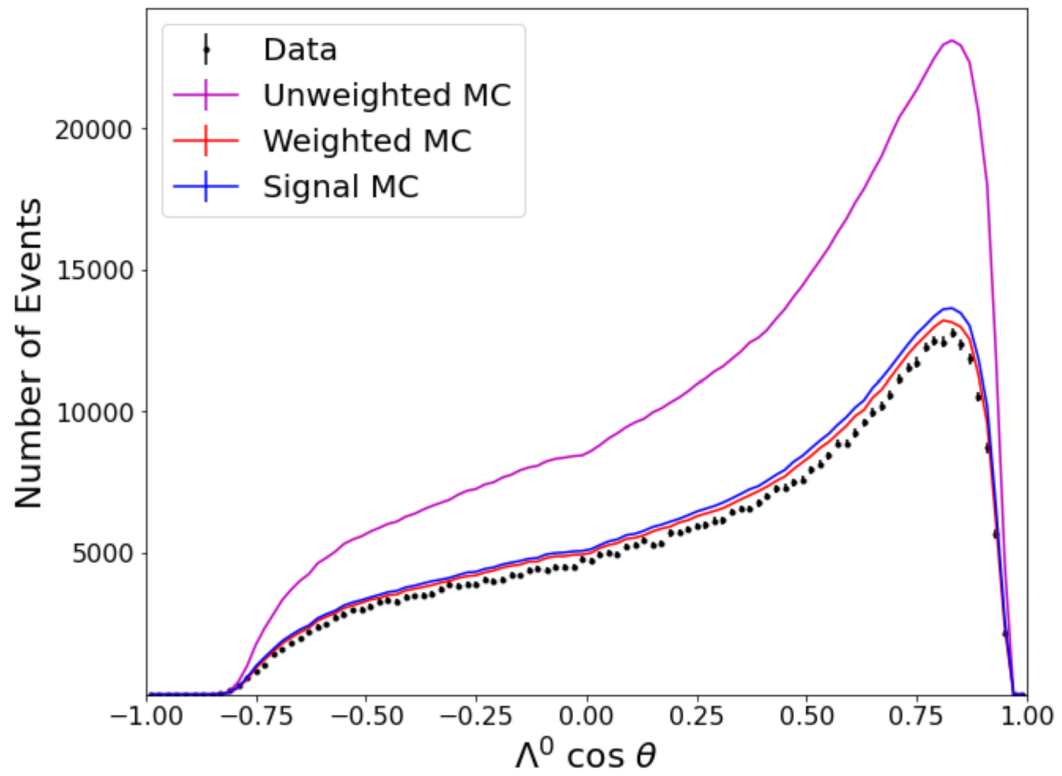


Figure 3.1 - Plot of the angular displacement of the Λ^0 baryon. The black markers represent the weighted data, the purple lines represent unweighted MC, the red line represents the weighted MC, and the blue line represents the signal in MC as determined from the truth information.

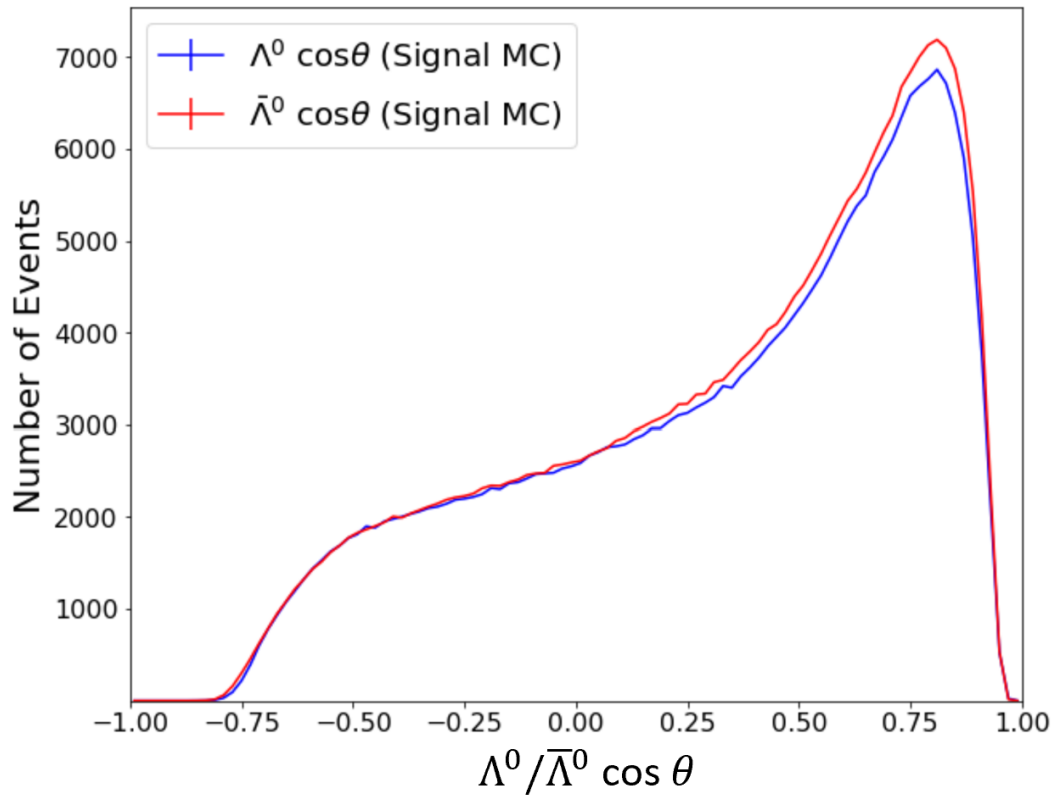


Figure 3.2 - Plot of the angular distribution between Λ^0 and $\bar{\Lambda}^0$ for signal MC. The blue line represents the Λ^0 distribution and the red line represents the $\bar{\Lambda}^0$ distribution. The forward bias is from the beam asymmetry.

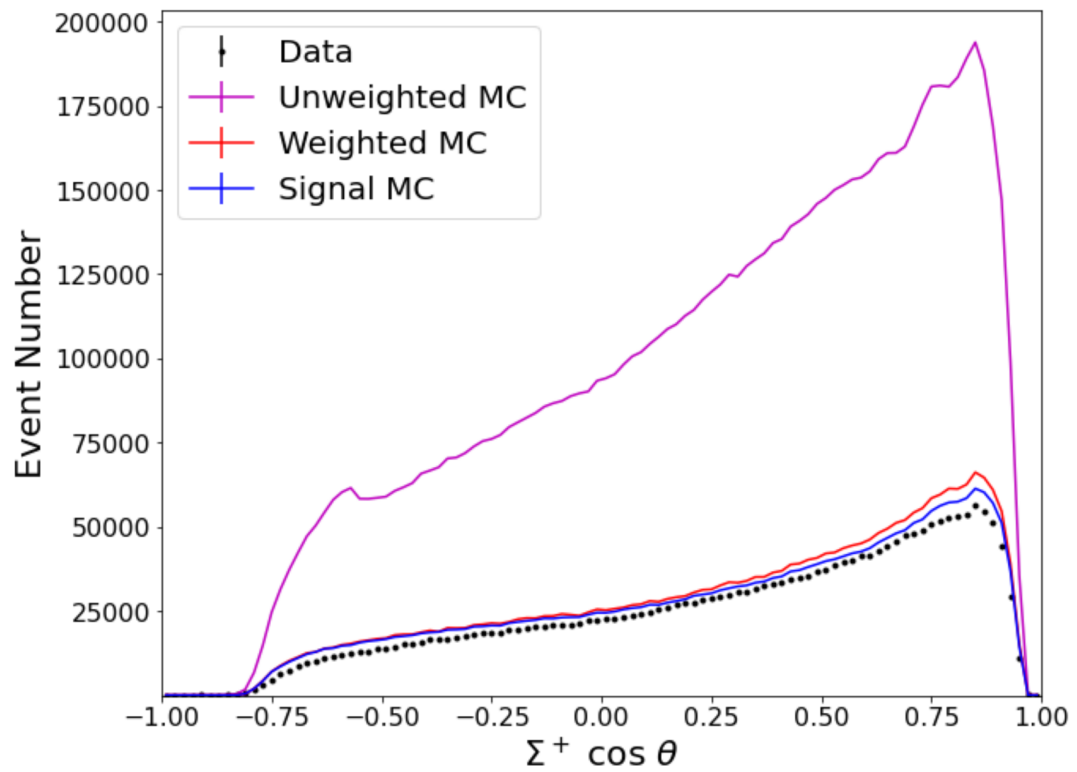


Figure 3.3 - Plot of the angular displacement of the Σ^+ baryon. The dotted lines represent data, the purple lines represent unweighted MC, the red line represents the weighted MC, and the blue line represents the signal. The vertical column represents event count. After applying weights, the weighted MC and signal MC strongly agree.

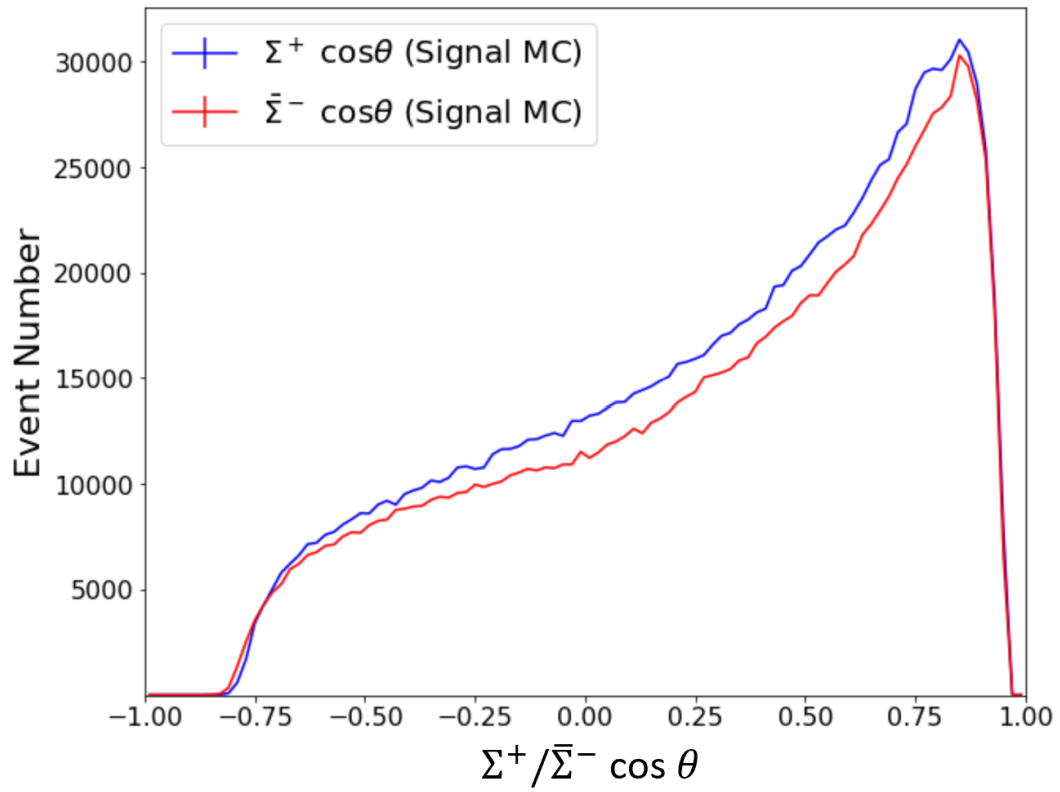


Figure 3.4 - Plot of the angular distribution between Σ^+ and $\bar{\Sigma}^-$ for signal MC. The blue line represents the Σ^+ distribution and the red line represents the $\bar{\Sigma}^-$ distribution. The forward bias is from the beam asymmetry.

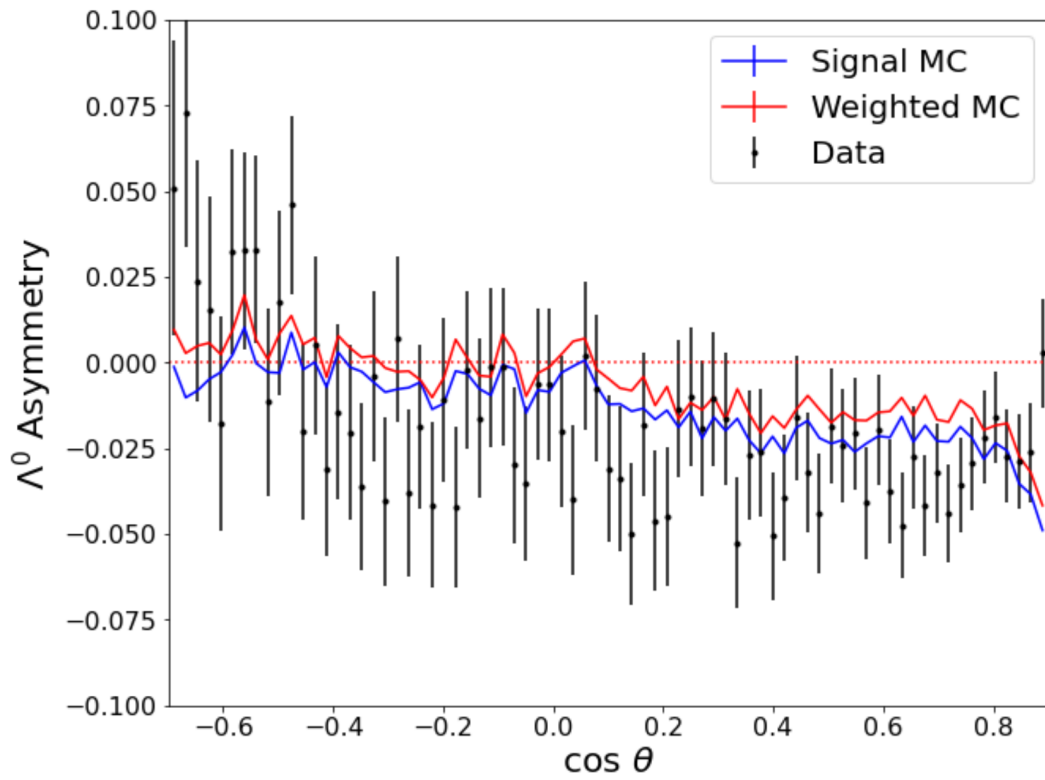


Figure 3.5 - A final measure of the the Λ^0 detection asymmetry with a dotted line at $y = 0$. The blue curve represents signal MC, the red curve represents the weighted MC and data, and the black points represent data points with statistical uncertainties.

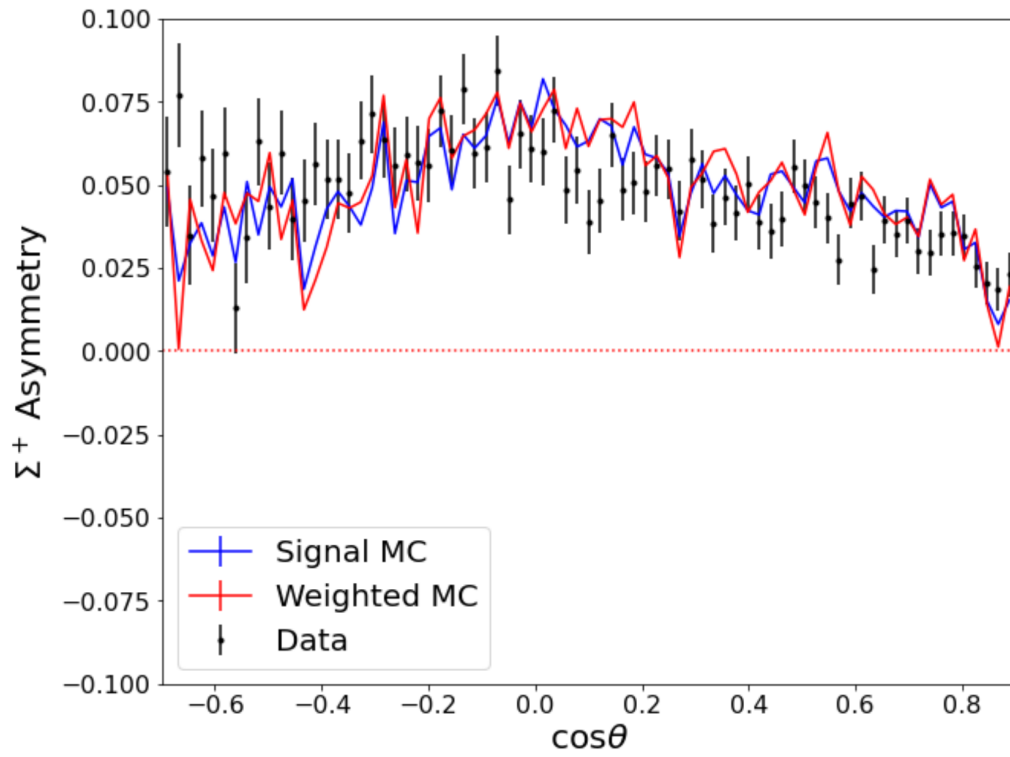


Figure 3.6 - A final measure of the the Σ^+ detection asymmetry with a dotted line at $y = 0$. The blue curve represents signal MC, the red curve represents the weighted MC and data, and the black points represent data points with statistical uncertainties.

4: Discussion

Baryon decays examined in this study are useful for analyzing raw asymmetry due to sources other than CP violation since they do not violate CP symmetry. MC is useful for recreating the conditions of a detector, allowing for a direct comparison where every decay can be accurately known. Removing background is essential to examining the decays of interest. In both decays, the weighted MC, signal MC, and weighted data all line up with reasonable precision in the asymmetry plots. Despite the difference in event count between MC and data for both decays, the asymmetry was determined with reasonable precision.

Asymmetry appears in both decays, but there appear to be differences in asymmetry. For Λ^0 , the raw asymmetry appears to be mostly neutral outside of the forward region of the detector, in which $\bar{\Lambda}^0$ is detected at a greater rate. As indicated by Figure 3.6, Σ^+ has a positive asymmetry, indicating that baryons are more readily detected by Belle II. This difference in asymmetry is not necessarily surprising, since Λ^0 is a neutral particle while Σ^+ is charged. However, this study only analyzed raw asymmetry. Since CP asymmetry is non-existent in this decay, there could be asymmetry due to production (i.e. the process of creating these particles causes some asymmetry).

Overall, this demonstrates a significant degree of detector asymmetry that must be accounted for in future studies and presents a potential future study. In order to accurately measure the violation of CP symmetry in any particle interaction, one must take into account internal bias from particle detection. The aim of this thesis was to study the baryon detection asymmetry in Belle II. The results of this study will have to be taken into account for future studies of CP violation at Belle II.

Bibliography

- [1] C. S. Wu et al., *Physical Review*. 105(4), 1413 (1957).
- [2] *Super KEKB and Belle II*. WWW document,
(https://www.belle2.org/project/super_kekb_and_belle_ii/).
- [3] T. Abe et al., *Belle II Technical Design Report*. (KEK, Tsukuba, 2010).
- [4] Giacomo De Pietro, *Generating Monte Carlo*. WWW document,
(https://software.belle2.org/sphinx/release-06-00-14/online_book/basf2/generating_mc.html#why-do-we-need-monte-carlo-simulated-data).
- [5] M. Pivik and F.R. Le Diberder, *Nuclear Instruments and Methods in Physics Research Section A: Accelerators, Spectrometers, Detectors and Associated Equipment*. 555(1-2), 359 (2005).
- [6] *zfit: scalable pythonic fitting*, WWW document,
(<https://zfit.readthedocs.io/en/latest/index.html>).
- [7] *Statistics tools and utilities*, WWW document, (<https://scikit-hep.org/hepstats/>).